p-ISSN 2089 – 0133 e-ISSN 2477-6416 Indonesian Journal of Applied Physics (IJAP) Vol. 14 No. 2 page 219
URL : https://jurnal.uns.ac.id/ijap/article/view/70654 DOI : https://doi.org/10.13057/ijap.v14i2.70654

REVIEW OF ELECTRICAL PARAMETERS INFLUENCE ON CHARACTERISTICS OF PLASMA ELECTROLYTIC OXIDE COATING ON ZIRCALOY

Fajar Al Afghani[1,2], Anawati Anawati[1*]
[1]Departemen Fisika, Fakultas Matematika dan ilmu Pengetahuan Alam, Universitas Indonesia, Depok, Indonesia
[2]Pusat Riset dan Teknologi Daur Bahan Bakar Nuklir dan Limbah Radioaktif, Badan Riset dan Inovasi Nasional, Serpong, Indonesia
[*]anawati@sci.ui.ac.id

Received 19-01-2023, Revised 03-01-2024, Accepted 01-09-2024,
Available Online 01-09-2024, Published Regularly October 2024

ABSTRACT

Zircaloy-4 (Zr-4) is used as a fuel cladding material in Pressurized Water Reactor (PWR). Zr-4 as a cladding material works in extreme conditions in pressurized water up to 150 atm at 325 ˚C. In addition, the refuelling process in the reactor requires surface protection of the clay material to minimize corrosion and wear. One of the raising methods to enhance the corrosion resistance of the Zr-4 is by plasma electrolytic oxidation (PEO). Characteristics of the ceramic oxide layer produced by PEO are influenced by current density, type and composition of the electrolyte, and voltage mode. One of the challenges in the PEO development on the Zr-4 substrate is a high porosity with a range of 5%-20% and the low number (below 6%) of t-ZrO_2 phases in the inner and outer layers. Optimizing the electrical parameters is necessary to overcome this problem. The results of the literature study show that the cathodic current at the AC voltage plays an important role in determining the resulting plasma characteristics. Low duty cycle (cathodic current> 50%) produce plasma with high density, resulting in a low porosity layer. Oppositely, high duty cycle (cathodic current <50%) produced high content of t-ZrO_2 increase the mechanical resistance. Two-step PEO is beneficial in combining the low and high duty cycle to obtain the benefit of each step.

Keywords: zircaloy; cladding; PWR; plasma electrolytic oxidation; frequency

Cite this as: Afghani, F. A., & Anawati. 2024. Review of Electrical Parameters Influence On Characteristics of Plasm Electrolytic Oxide Coating On Zircaloy. *IJAP: Indonesian Journal of Applied Physics, 14*(2), 219-233. doi: https://doi.org/10.13057/ijap.v14i2.70654

INTRODUCTION

In 2022, the International Atomic Energy Agency (IAEA) reported that 68% of nuclear power plants worldwide utilize pressurized water reactors (PWR)[1]. A crucial component of PWR is the nuclear fuel cladding, which is made of a zirconium (Zr) alloy. This cladding serves as a level I protector, preventing the escape of radioactive substances from fission reactions into the environment. Figure 1 illustrates the historical development of Zr alloys for fuel cladding in pressurized power reactors[2–4]. Initially, Zr alloys such as Zr-1Sn-1Nb, Zr-2.5Nb, Zr-1Nb, and zircaloy-2 (Zr-2) were used for nuclear applications. The addition of Cr and Ni to the Zr alloy, specifically Zr-2 alloy, is sufficient for nuclear reactors with water vapor at a pressure of 1 atm due to the performance of Cr which can withstand corrosion at low temperatures. However, as PWR nuclear reactors developed, their thermal efficiency surpassed 40%, surpassing that of boiling water reactors (BWR) with a thermal efficiency below 35%. This led to the demand for cladding materials with higher corrosion resistance under high pressures. To enhance the corrosion resistance of Zr alloy-based cladding material for PWR, a modification was made by

eliminating the Ni element and reducing the Sn concentration to a maximum of 1.3%. This adjustment effectively reduces grain boundary corrosion that occurs at high pressures. As a

result, a commercially produced cladding material called zircaloy-4 (Zr-4) was developed. Zr-4 consists of alloying elements 1.5 wt.% Sn, 0.2 wt.% Fe, and 0.1 wt.% Cr. This alloy is specifically chosen for PWR fuel cladding due to its impressive corrosion resistance and reliable mechanical properties, even under pressures exceeding 150 atm[5]. While Zr-4 exhibits decent corrosion resistance, it is prone to high-temperature corrosion because of fuel burn-up in reactors with an efficiency of over 40%. Additionally, researchers are currently grappling with the issue of fretting wear during the refuelling process, which poses a challenge to enhancing the performance of PWR nuclear fuel cladding. The ultimate goal is to achieve zero failures in the cladding material[6]. The corrosion and wear resistance of a material can be enhanced through the optimization of its chemical composition and surface treatment methods[7].

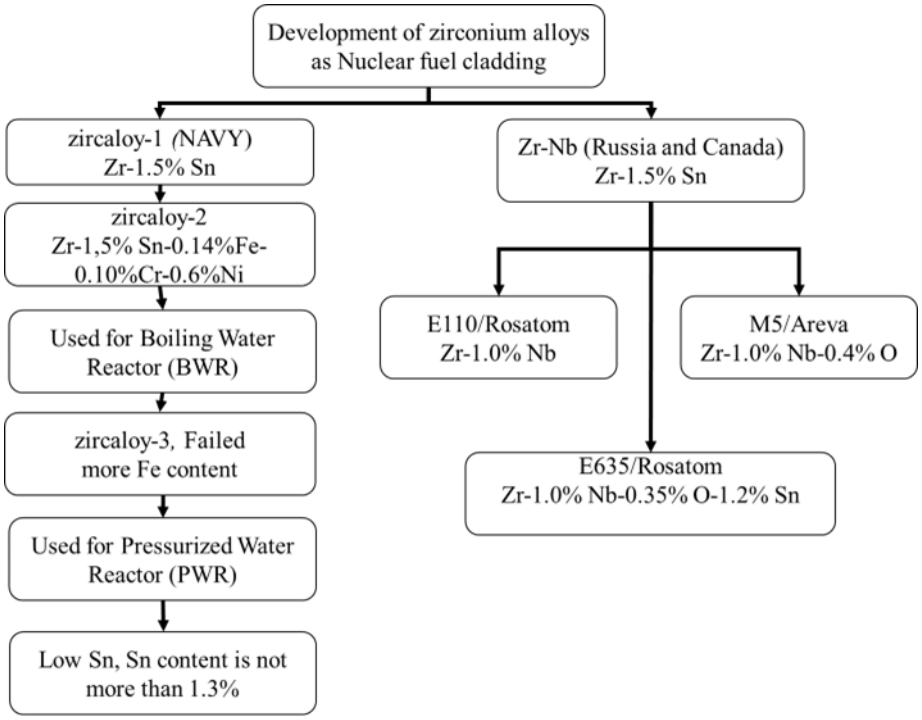

Figure 1. Developments in the use of zirconium alloys for nuclear fuel cladding

Various coating methods have been employed on Zr-4, including electroplating[8], Physical Vapor Deposition (PVD)[9], Chemical Vapor Deposition (CVD) [10], and Plasma Electrolytic Oxidation (PEO) [11–13]. However, Electroplating generates heavy metal waste[14]. PVD and CVD, on the other hand, involve high operating costs due to the need for a vacuum[15], and long processing times[16]. In contrast, PEO represents an environmentally friendly approach for growing ceramic oxide coatings. The PEO process utilizes an alkaline salt-based solution and does not require a vacuum or extensive coating time. Essentially, PEO involves anodizing metals in alkaline salt electrolytes using a high-power supply to excite plasma on the metal surface, transforming it into an oxide ceramic. Extensive research has been conducted on coating formation mechanisms and characteristics in aluminium (Al) [17]–[21], magnesium (Mg) [22–24], titanium (Ti) [25–28], and zirconium (Zr) [29]. The results have demonstrated significant

improvements, including a 100-fold increase in corrosion resistance, a 20-fold increase in wear resistance, and a 2-3 times enhancement in surface hardness compared to the substrate[30].

The appearance of plasma is influenced by both the electrical parameters and electrolyte composition. An electrolyte with a higher electrical conductivity requires less electric field to generate plasma[31]. At a low DC current density of 30 – 70 mA/cm^2, plasma can be generated at 150 V in an electrolyte containing 30 g/l Na_3PO_4 + 30 g/l Na_2SiO_3 + 30 g/l KOH[32]. The PEO layer, especially the inner part, is rich in SiO_2 as a result of deposition of the electrolyte substance, while the outer layer contains a balanced ratio of SiO_2/ZrO_2 as a result of inward and outward growth of the oxide layer. At a high current density using AC mode, the PEO layer had a balance SiO_2/ZrO_2 and similar composition between the inner and outer layers[33]. The impact of frequency ranging from 28 Hz to 10457 Hz on the coating properties of the Zr alloy has been studied[34]. The results of frequency optimization indicate that a frequency of 3137 Hz yields a 6% t-ZrO_2 phase. However, the impact of frequency on the percentage of pores, which can affect the corrosion resistance of Zr-4 alloy, has not been analyzed. Hence, this study focuses on the advancement of PEO research on Zr-4, specifically investigating the influence of AC electrical parameters on coating morphology and composition. The objective is to obtain optimal electrical parameters for the Zr-4 AC-PEO process based on this literature review.

METHOD

This research used literature study method to gather information from the reliable sources including journals, books, and proceedings. The schematic diagrams prepared in this work were based on the analysis from several publication resources with the main purpose to give a better understanding on the discussed topics.

Mechanism of plasma electrolytic oxidation (PEO) in zirconium alloys

Figure 2 illustrates the PEO equipment. The set up consists of power supply as a current/voltage source, the electrochemical cell, and multimeter for measuring the current/voltage output. The electrochemical cell consisted of specimen as anode and an inert electrode as cathode. Cooling system is required to maintain the electrolyte temperature stable because during plasma generation, the local temperature in the electrolyte raises significantly. The electrolyte for PEO on Zr uses acid, alkaline, or salt-based electrolyte. The resulting PEO coatings composed of metal cation and anion from the electrolyte. When employing a salt-based electrolyte, such as Na_2SiO_3, the resulting PEO coating comprises of SiO_2 and ZrO_2[35].

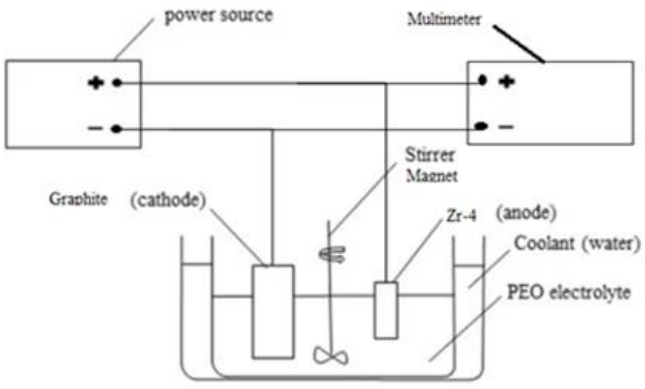

Figure 2. Schematic diagram of PEO equipment

Figure 3 illustrates the mechanism behind the formation of PEO layers, which occurs through four stage [36]. In stage I, there is a rapid and linear increase in voltage over time. This initial stage represents the general anodization, where metal ions are released from the sample's surface due to charge polarization. As metal ions accumulate and undergo hydrolysis, they reach a saturation state and deposit on the surface, forming a thin layer called a barrier layer. The thickness of the barrier layer, ranging from 40 to 940 nm, depends on the electrolyte and electrical parameters applied[37–39]. The charges continue to accumulate on the dielectric barrier layer with time. When the electric field reaches 3 – 30 MV/m, leakage of the dielectric layer occurs[40]. In Stage II, when the applied voltage surpasses the breakdown value, dielectric breakdown occurs, resulting in plasma spark discharge. Small white plasma sparks appear to flash on the metal surface. White plasma has a temperature of 4000 -5000 K with an intensity of 100-200 sparks/ms[41,42]. The plasma is formed through the tunnelling of electrons from the dielectric layer. However, another theory suggests that plasma is generated by a cloud layer surrounding the metal surface when a high electric field is reached, the cloud layer triggers a plasma spark through the dielectric layer, similar to natural lightning phenomena[43]. In this stage, current flow becomes concentrated in the damaged area, forming a tunnel. Within the plasma, a thermo-chemical and metallurgical reaction takes place between the molten metal from the substrate and ions from the electrolyte, resulting in the formation of molten oxide. The high pressure within the plasma expels the molten oxide from the bottom, propelling it onto the surface. This event is analogous to a volcanic eruption expelling hot lava. As the coating thickens, it becomes more challenging to excite the plasma. Consequently, the voltage continues to rise until it reaches a critical voltage range of 250-570 V for zirconium-based metals[44,45]. At this critical voltage, locally emitted plasma exhibits a higher intensity. The colour of the plasma changes to orange or reddish. In stage III, continuous melting, and oxide layer formation cause fluctuations in cell potential. Stage IV is characterized by the formation of an electrical cloud comprising both positive and negative ions, which become trapped as they are unable to penetrate the thicker oxide layer. The release of gases and vigorous splashing leads to the creation of large pores and cracks in the oxide layer. Some of these ions can recombine into gas, triggering the production of additional large pores and cracks. Moreover, when provided with continuous electrical energy, some of these ion clouds can once again induce plasma sparks with softer characteristics. These sparks exhibit smaller sizes but occur simultaneously both inside and outside the oxide layer. Some researchers refer to this plasma stage as soft plasma[46].

The plasma emitted during PEO can be observed using various instruments, including an oscilloscope to record waveform, voltage, current, and frequency data, as well as a high-speed camera to capture the shape, size, and duration of the plasma. These tools facilitate the generation of soft plasma profile data during the PEO process.

The discrepancies between PEO stages when using DC and AC voltage sources are only noticeable on a micro time scale, specifically in the range of milliseconds. PEO with an AC voltage source involves fluctuating positive and negative voltage and current values. On the other hand, PEO with a DC voltage source does not exhibit negative voltage or current.

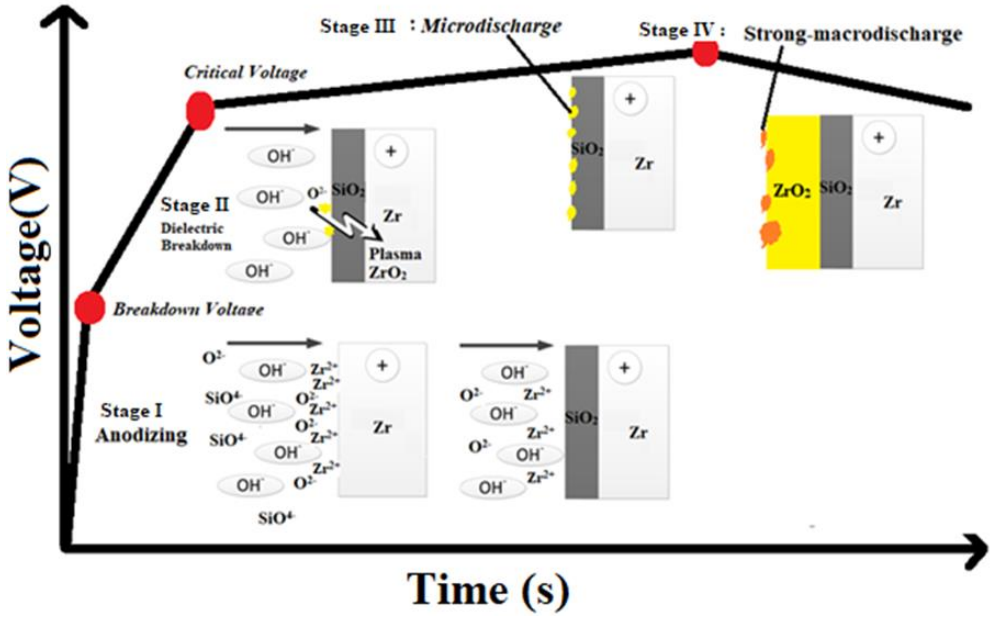

Figure 3. Illustration stages in PEO as a function of time using constant DC current mode

Effective parameter on PEO in general

Figure 4 demonstrates the influential parameters that affecting the properties of PEO coating. The electrolyte composition and substrate material are two intrinsic factors crucial for achieving the desired microstructure and phase composition of the coating[47]. The electrolyte contains anions and cations that involves in the formation of the oxide layer. The type of electrolyte affected the properties of the deposited layer, including pore size, morphology, constituent phases, and corrosion resistance. Electrolytes containing aluminate, silicate and phosphate are commonly employed to enhance the coating properties of Zr alloys[48]. Silicate-based electrolytes with concentrations of 16, 31, 48, and 56 g/L resulted in growth rates of 2.3, 2.6, 2.9, and 9.7 μm/min during the PEO process[49].

Low temperatures (below 20 ˚C) promote the stabilization of the t-ZrO_2 crystalline phase as they accelerate solidification. However, temperatures below 10 ˚C result in weak oxidation, yielding a thin layer with lower hardness, approaching the substrate hardness value in the range of approximately 164-200 HV for Zr-4 hardness[50–52]. High temperatures (above 20˚C) increase the dissolution of the oxide film, significantly reducing the coating thickness and hardness to around 10-20 μm[53,54]. Therefore, the processing temperature for zircaloy is maintained within 10 ℃. The PEO duration directly affects the layer thickness, with a critical

limit of 90 min. Longer than the critical time, the coating is dissolved back to the electrolyte[55]. Moreover, the increased resistance to layer formation as the thickness of the layer increases, ultimately halting the oxidation process because no more metal ions are being released from the substrate to form plasma[55]. Furthermore, longer coating times lead to higher porosity in the outermost layer, exceeding 20%[56]–[61] and a greater number of cracks[62–65]. Hence, optimizing the processing time is crucial to achieve coating characteristics with minimal pores and cracks.

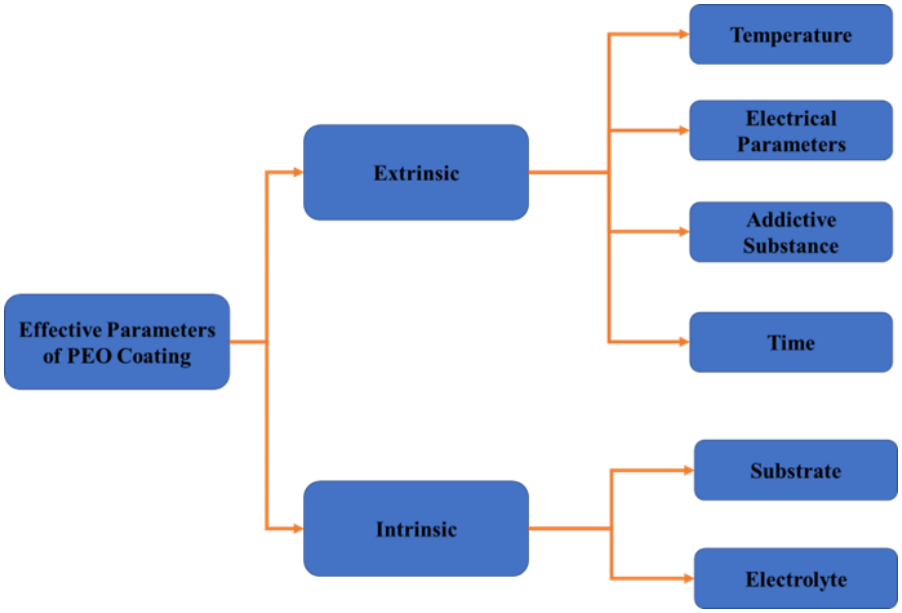

Figure 4. PEO parameters

RESULTS AND DISCUSSION

Development of PEO on Zr alloy

The application of PEO technology for coating has a long history, dating back to 1970 when Brown coated an Al substrate with a mixture of $NaAlO_3$ and Na_2SiO_3 solutions[66]. Since then, PEO techniques have been developed for other metals such as Al, Mg, and Ti[25], with a focus on enhancing corrosion and wear resistance[67–71]. However, the application of PEO for coating Zr alloy, specifically as a nuclear fuel cladding material, started in the early 2000s. Juan et al.[72] conducted PEO coating on Zr-4 using a DC voltage in NaOH electrolyte, resulting in a 4.7 µm thick coating and a corrosion current density of 0.018 µA/cm2. Pauporte et al.[73] also used a DC voltage to produce a 3.2 µm thick ZrO_2 layer on Zr metal, achieving a Faraday efficiency of 25%. Chen investigated the effect of pulsed DC voltage with a frequency of 2000 Hz, which increased the wear resistance by nearly 2 times compared to the substrate[74]. Zhou et al.[75], Matykina et al[76]and W. Xue et al.[77] employed an AC power source in Na_2SiO_3 electrolyte to create wear-resistant ZrO_2 coatings on Zr alloy. Researchers have found that the characteristics of PEO coatings depend on various process parameters, including electrolyte composition, current density, and time. Several studies focusing on improving corrosion properties of PEO coatings on Zr alloys are summarized in Table 1.

Table 1 presents the application of PEO for coating Zr alloys using a mixture of sodium silicate (Na_2SiO_3), sodium phosphate, and potassium hydroxide. The addition of Na_2SiO_3 electrolyte enhances the coating's growth rate[81]. Sodium phosphate (Na_3PO_4) electrolyte, on the other hand, plays a crucial role in stabilizing the distribution of plasma. It acts as a buffer solution, maintaining the solution's conductivity stable. As a result, the voltage deviation during stages 2 and 3 on the Vt curve is only around ±5-10 V, compared to using only sodium silicate (Na_2SiO_3) which exhibits a larger deviation of ±100-250 V[82].

Table 1. History of PEO coatings on zirconium alloys and the characteristics of the resulting coatings

Researcher	Substrate type	PEO Parameters			Layer Characteristics	
		Electrolyte	voltage type	Electrical parameters	ZrO_2 crystalline phase composition	Layer morphology/porosity/crack/thickness
Juan et al., 2005[72]	Zr-4	NaOH	DC	i = 100 mA/cm^2	m-ZrO_2 = 99% t-ZrO_2 = 1%	4.7 µm thick, Surface pores not clearly visible. Crack at many latitudes
Ying Chen et al., 2010)[78]	Zr-2.5% Nb	0,8 g/L KOH + 8 g/L Na_2SiO_3	pulsating DC	i = 250 mA/cm^2	Tidak dihitung	Thickness 5.3 – 5.7 µm, very little surface porosity (<1%), very dense cross section, little crack
Matykina et al., 2010[79]	zirloTM	2,8 g/L KOH + 30 g/L Na_2SiO_3	Bipolar AC	i = 100 mA/cm^2	m-ZrO_2 = 98% t-ZrO_2 = 2%	5 µm thick There are no pores on the inner layer but many pores are found on the outer layer
Xue et al., 2010[77]	Zr-2.5% Nb	Na_2SiO_3 +KOH	Bipolar AC	200 V	m-ZrO_2 = 98% t-ZrO_2 = 2%	25 -240 µm thick, 25 µm thick has more pores than 240 µm thick both on the surface and cross section
YM Wang et al., 2018[80]	Zr-4	3 g/L KOH + 10 g/L Na_2SiO_3	Bipolar AC	V= 550 V	m-ZrO_2 = 97% t-ZrO_2 = 1%	4 – 5 µm thick, many pores and pancakes are found on the surface but in cross-section the layer appears to be non-porous
Parthenov, 2019[34]	Zr-1Nb	1 g/L KOH +2 g/L Na_2SiO_3	Unipolar AC	V= 570 V	m-ZrO_2 = 94% t-ZrO_2 = 6%	10 – 15 µm thick, the higher the frequency applied the fewer pores on the surface
Malayoğlu et al., 2020[13]	Zr-702	12 g/L KOH + 12 g/L Na_2SiO_3	Bipolar AC	i = 200 mA/cm^2	m-ZrO_2 = 100% t-ZrO_2 = 0%	Thickness of 120 µm, the longer the PEO time the more pores on the surface but the fewer pores on the cross section
Na Li et al., 2021[81]	Zr-2	1 g/L KOH + 8 g/L Na_2SiO_3	Bipolar AC	i = 150 mA/cm^2	m-ZrO_2 = 95% t-ZrO_2 = 5%	Thickness of 70 -78 µm, increasing the concentration of Na_2SiO_3 can reduce the porosity on the surface and cross section

i = current density; V=voltage

Effect of Stress Mode on the Characteristics of the PEO Zr-4 layer

Pulsed AC and DC mains modes offer greater control over the chemical processes of plasma compared to normal DC modes, resulting in more uniform coatings with reduced porosity and strong adhesion to the substrate[83]. Researchers have also explored the influence of the hybrid mode (AC+DC) to investigate the microstructure and properties of PEO coatings[84,85]. Yonghao[86] compared the differences in the characteristics of the PEO layer with the AC and DC voltage modes where the PEO layer with the AC voltage mode has fewer pores but is

thinner. Additionally, PEO coatings formed with AC voltage can effectively cover pores that may have been caused by hydrogen gas trapped during the cooling process. In the AC voltage mode, the pores in the plasma discharge channel can be effectively closed due to the interaction between the negative current and positive ions from the substrate. This reaction occurs with the negative electrolyte ions that originate from the trapped gas evolution within the discharge channel[87]. AC voltage, particularly with bipolar pulses, has a negative voltage component that helps reduce the trapped hydrogen gas[88]. This is opposite with the DC voltage mode, which

applies a continuous positive voltage during layer formation, leading to the accumulation of hydrogen gas and the formation of pores within the PEO layer.

During the PEO process, hydrogen gas is generated due to the electrolysis of water. This gas becomes trapped within the plasma formation channel, also known as the discharge channel. In the DC voltage mode, continuous plasma formation prevents a significant amount of hydrogen gas from cooling down and returning to the electrolyte solution. As a result, the trapped hydrogen gas contributes to the formation of pores, as depicted in Figure 5.

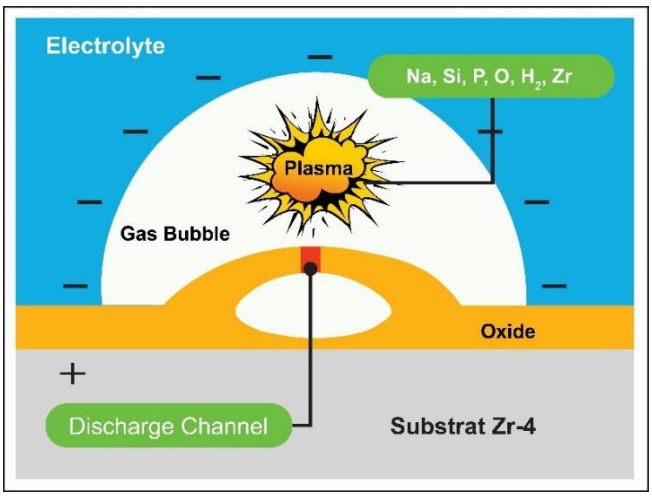

Figure 5. Illustration of gas bubbles formation during PEO

Oxide films can be generated through AC current or continuously pulsed bipolar regimes, utilizing both positive and negative waveform values. These conditions result in slower layer formation but significantly increased hardness. Arrabal et al.[89] observed that pore closure can form during the PEO process using the AC regime when the voltage is on the negative cycle. Basically, the change in voltage after stage 3 is associated with a decrease in intensity and the appearance of micro-charges, which is referred to as soft sparking. Interestingly, according to research by Matykina et al.[79] the phenomenon of soft sparking, which utilizes AC voltage and a silicate electrolyte, occurs in stage 3 and after a prolonged processing time.

Effect of electrical parameters on AC voltage on the characteristics of the PEO layer

The PEO coating process using AC voltage mode is affected by various electrical parameters, including the phase between voltage and current density, duty cycle, frequency, and waveform. This study aims to explore the impact of these electrical parameters on the morphology, thickness, mechanical properties, and corrosion resistance of the PEO coating. The surface morphology and cross-section of the PEO coating are crucial characteristics as they determine the thickness, uniformity, and porosity, which directly influence its mechanical properties and corrosion resistance. Previous studies have demonstrated that porosity exhibits an inverse linear relationship with wear and a logarithmic inverse relationship with corrosion

resistance[90]. This is due to a high percentage of pores, which increases surface friction and susceptibility to abrasion, resulting in lower wear rates[91]. Additionally, the presence of a significant number of pores in the coating facilitates corrosion reactions between the substrate and the electrolyte in the surrounding environment through these pores. The following discussion will delve into the influence of electrical parameters in the PEO process using AC voltage mode on the characteristics of the resulting PEO layer.

a. Duty cycle

The duty cycle represents the duration of the high voltage period in a signal period and is expressed as a percentage ranging from 0% to 100%. A low duty cycle corresponds to higher maximum voltage and plasma voltage. When a duty cycle below 50% is applied, it leads to micro-discharges with higher spatial density but lower intensity. These milder micro-discharges result in smaller craters. On the other hand, applying a duty cycle above 50% during the PEO process causes the plasma to increase in size but decrease in quantity, particularly with longer durations. Dehnavi[92] conducted research on the impact of low (<50%) and high (>50%) duty cycles on the distribution of silicon elements derived from Na_2SiO_3 electrolytes. The findings of these studies revealed that the behaviour of the plasma, influenced by different electrical parameters, affects the distribution of silicon. A duty cycle below 50% leads to a lower concentration of Si on the surface and a more uniform distribution of Si throughout the coating. This phenomenon can be attributed to the higher plasma density associated with a duty cycle below 50%[26].

b. Frequency

Higher applied frequencies in the PEO process result in fewer surface pores and a more uniform phase distribution on the surface. This is because the alternating voltage and high frequency help to cover partially closed channels formed during the PEO process[93]. However, the difference becomes less significant with a very wide frequency range. Parfenov[34] conducted research on the phase composition of ZrO_2 produced in the PEO process of zirconium alloy using different frequency parameters. According to Table 2, increasing the applied frequency leads to an increase in the corrosion potential of the zirconium alloy, indicating higher corrosion resistance. At higher frequencies, the t/m- ZrO_2 phase ratio is greater compared to lower frequencies. This is because the high-frequency AC voltage restricts the formation of the t- ZrO_2 phase, which typically occurs at high temperatures. Sabouri[94] added that the t- ZrO_2 crystal structure has a higher atomic density, making it more resistant to corrosion reactions.

Table 2. the effect of the applied frequency on the corrosion properties and the phases formed in the zirconium alloy[34]

Frequency (Hz)	Corrosion characteristics		XRD Analysis Results (%)		
	E_{corr} (V)	I_{corr} (10-4 A/m2)	α-Zr	m- ZrO_2	t- ZrO_2
0	-0.15	29.0	100	-	-
62	-0.11	13.0	-	97	3
713	-0.11	4,5	-	95	5
3137	-0.08	4.0	-	94	6

CONCLUSION

Based on the literature review, the following conclusions are made: Combination of alkaline salts Na_2SiO_3, Na_3PO_4, and KOH is preferable to obtain the benefit of each ions in producing better PEO coatings performance on Zr-4. Silicate ions produce SiO_2, improving wear resistance. Phosphate ions triggers strong plasma generation, creating higher crystalline oxide product. KOH electrolyte has a higher solution conductivity, enabling immediate plasma formation at a low voltage. The electrolyte temperature should be maintained between 5-10˚C to facilitate solidification and promote the formation of a crystalline phase on the oxide layer. The recommended AC voltage mode for PEO on zircaloy is bipolar voltage with a range of 50-

570 V_{rms}. This allows for better observation of the fine plasma, which plays a crucial role in determining layer quality. Duty cycle in the range of 25-75% is suitable for the PEO process on zircaloy. Lower duty cycles result in microdischarges with higher spatial density but lower intensity, while higher duty cycles produce stronger micro plasma discharges with reduced quantity, particularly over longer durations. And frequencies ranging from 50-500 Hz are found to be most effective for the PEO process.

ACKNOWLEDGMENTS

The author would like to thank to the Degree by research program BRIN.

REFERENCES

1 International Atomic Energy Agency. 2021. *World Nuclear Performance Report 2021* (Report No. 2021/003).
2 Allen, T. R., Konings, R. J. M., Motta, A. T., & Couet, A. 2020. Corrosion of zirconium alloys. In R. J. M. Konings & R. E. B. T.-C. N. M. (Eds.), *Comprehensive nuclear materials* (2nd ed., pp. 64–95). Elsevier.
3 Young, G. A., Hackett, M. J., Tucker, J. D., & Capobianco, T. E. 2020. Welds for nuclear systems. In R. J. M. Konings & R. E. B. T.-C. N. M. (Eds.), *Comprehensive nuclear materials* (2nd ed., pp. 517–544). Elsevier.
4 Onimus, F., Doriot, S., & Béchade, J.-L. 2020. Radiation effects in zirconium alloys. In R. J. M. Konings & R. E. B. T.-C. N. M. (Eds.), *Comprehensive nuclear materials* (2nd ed., pp. 1–56). Elsevier.
5 Yang, M., Gao, Y., & Wang, H. 2020. Effect of $Zn(CH_3COO)_2$ addition on corrosion of Zirlo alloy in simulated PWR primary loop medium with LiOH and H_3BO_3. *Journal of the Chinese Society for Corrosion and Protection*, 40(2), 199–204.
6 Suman, S. 2019. Burst criterion for Indian PHWR fuel cladding under simulated loss-of-coolant accident. *Nuclear Engineering and Technology*, 51(6), 1525–1531.
7 Kaufholz, P., Stuke, M., Boldt, F., & Péridis, M. 2018. Influence of kinetic effects on terminal solid solubility of hydrogen in zirconium alloys. *Journal of Nuclear Materials*, 510, 277–281.
8 Luscher, W. G., Gilbert, E. R., Pitman, S. G., & Love, E. F. 2013. Surface modification of Zircaloy-4 substrates with nickel zirconium intermetallics. *Journal of Nuclear Materials*, 433(1–3), 514–522.
9 Umretiya, R. V., Elward, B., Lee, D., Anderson, M., Rebak, R. B., & Rojas, J. V. 2020. Mechanical and chemical properties of PVD and cold spray Cr-coatings on Zircaloy-4. *Journal of Nuclear Materials*, 541, 50–65.
10 Diniasi, D., Golgovici, F., Anghel, A., Fulger, M., Surdu-Bob, C. C., & Demetrescu, I. 2021. Corrosion behavior of chromium-coated Zy-4 cladding under CANDU primary circuit conditions. *Coatings*, 11(11), 1417.
11 Mengesha, G. A., Chu, J. P., Lou, B. S., & Lee, J. W. 2020. Effects of processing parameters on the corrosion performance of plasma electrolytic oxidation grown oxide on commercially pure aluminum. *Metals*, 10(3), 1–21.
12 Cheng, Y., Wang, T., Li, S., Cheng, Y., Cao, J., & Xie, H. 2017. The effects of anion deposition and negative pulse on the behaviours of plasma electrolytic oxidation (PEO)—A systematic study of the PEO of a Zirlo alloy in aluminate electrolytes. *Electrochimica Acta*, 225, 47–68.
13 Malayoğlu, U., Tekin, K. C., Malayoğlu, U., & Belevi, M. 2020. Mechanical and electrochemical properties of PEO coatings on zirconium alloy. *Surface Engineering*, 36(8), 800–808.
14 Ramrakhiani, L., Ghosh, S., & Majumdar, S. 2022. Heavy metal recovery from electroplating effluent using adsorption by jute waste-derived biochar for soil amendment and plant micro-fertilizer. *Clean Technologies and Environmental Policy*, 24(4), 1261–1284.
15 Latchford, I., Riposan, A., Kudriavtsev, V., Bluck, T., & Smith, C. 2015. Cost of ownership

analysis for a high productivity thin film PVD system. In *Society of Vacuum Coaters 57th Annual Technical Conference Proceedings* (Vol. 57, pp. 516–519).

16 Bao, W., Xue, J., Liu, J. X., Wang, X., Gu, Y., Xu, F., & Zhang, G. J. 2018. Coating SiC on Zircaloy-4 by magnetron sputtering at room temperature. *Journal of Alloys and Compounds*, *730*, 81-87.Agureev,

17 Agureev, L., Savushkina, S., Ashmarin, A., Borisov, A., Apelfeld, A., Anikin, K., ... & Bogdashkina, N. 2018. Study of plasma electrolytic oxidation coatings on aluminum composites. *Metals*, *8*(6), 459..

18 Huang, X. 2019. Plasma electrolytic oxidation coatings on aluminum alloys: Microstructures, properties, and applications. *Modern Concepts in Material Science*, 2(1).

19 Jadhav, P., Bongale, A., & Kumar, S. 2021. A review of process characteristics of plasma electrolytic oxidation of aluminium alloy. *Journal of Physics: Conference Series*, 1854(1).

20 Dehnavi, V., Shoesmith, D. W., Luan, B. L., Yari, M., Liu, X. Y., & Rohani, S. 2015. Corrosion properties of plasma electrolytic oxidation coatings on an aluminium alloy - The effect of the PEO process stage. *Materials Chemistry and Physics*, 161, 49–58.

21 Lu, C., Ding, J., Shi, P., Jia, J., Xie, E., & Sun, Y. 2022. Effects of texture density on the tribological properties of plasma electrolytic oxidation/polytetrafluoroethylene coatings formed on aluminum alloys. *Macromolecular Materials and Engineering*, 307(2), 2100678.

22 Anawati, A., Asoh, H., & Ono, S. 2017. Effects of alloying element Ca on the corrosion behavior and bioactivity of anodic films formed on AM60 Mg alloys. *Materials*, 10(1).

23 Anawati, A., Asoh, H., & Ono, S. 2018. Degradation behavior of coatings formed by the plasma electrolytic oxidation technique on AZ61 magnesium alloys containing 0, 1, and 2 wt% Ca. *International Journal of Technology*, 9(3), 622–631.

24 Anawati, A., Hidayati, E., & Labibah, H. 2021. Characteristics of magnesium phosphate coatings formed on AZ31 Mg alloy by plasma electrolytic oxidation with improved current efficiency. *Materials Science and Engineering: B, Solid-State Materials for Advanced Technology*, 272, 115354.

25 Simchen, F., Sieber, M., Kopp, A., & Lampke, T. 2020. Introduction to plasma electrolytic oxidation—An overview of the process and applications. *Coatings*, 10(7), 1–19.

26 Lederer, S., Lutz, P., & Fürbeth, W. 2018. Surface modification of Ti 13Nb 13Zr by plasma electrolytic oxidation. *Surface Coatings Technology*, 335, 62–71.

27 Gowtham, S., Hariprasad, S., Arunnellaiappan, T., & Rameshbabu, N. 2017. An investigation on ZrO_2 nanoparticle incorporation, surface properties and electrochemical corrosion behaviour of PEO coating formed on CP-Ti. *Surface Coatings Technology*, 313, 263–273.

28 Yang, C., Cui, S., Wu, Z., Zhu, J., Huang, J., Ma, Z., ... & Wu, Z. 2021. High efficient co-doping in plasma electrolytic oxidation to obtain long-term self-lubrication on Ti6Al4V. *Tribology International*, *160*, 107018.

29 Ćirić, A., & Stojadinović, S. 2019. Photoluminescence studies of ZrO_2^{3+}/Yb^{3+} coatings formed by plasma electrolytic oxidation. *Journal of Luminescence*, 214.

30 Karimi, M., Boroujeny, B. S., & Adelkhani, H. 2022. Investigation and characterization of the plasma electrolytic oxidation of zirconium alloy: Effect of negative duty cycle. *Applied Physics A: Materials Science & Processing*, 128(8), 1–12.

31 Xu, W., Lu, X., Zhang, B., Liu, C., Lv, S., Yang, S., & Qu, X. 2018. Effects of porosity on mechanical properties and corrosion resistances of PM-fabricated porous Ti-10Mo alloy. *Metals*, *8*(3), 188.

32 Al Afghani, F., & Anawati, A. 2021. Plasma electrolytic oxidation of Zircaloy-4 in a mixed alkaline electrolyte. *Surface Coatings Technology*, 426, 127786.

33 Farrakhov, R. G., Mukaeva, V. R., Fatkullin, A. R., Gorbatkov, M. V., Tarasov, P. V., Lazarev, D. M., ... & Parfenov, E. V. 2018, January. Plasma electrolytic oxidation treatment mode influence on corrosion properties of coatings obtained on Zr-1Nb alloy in silicate-phosphate

electrolyte. In *IOP Conference Series: Materials Science and Engineering* (Vol. 292, p. 012006). IOP Publishing.

34 Parfenov, E. V., et al. 2019. Effect of frequency on plasma electrolytic oxidation of zirconium in pulsed unipolar mode. *IOP Conference Series: Materials Science and Engineering*, 672(1), 012010.

35 Aubakirova, V., Farrakhov, R., Astanin, V., Parfenov, E., Sharipov, A., & Gorbatkov, M. 2022. Plasma electrolytic oxidation of Zr-1%Nb alloy: Effect of sodium silicate and boric acid addition to calcium acetate-based electrolyte. *Materials*, 15(6).

36 Martin, J., Haraux, P., Ntomprougkidis, V., Migot, S., Bruyère, S., & Henrion, G. 2020. Characterization of metal oxide micro/nanoparticles elaborated by plasma electrolytic oxidation of aluminium and zirconium alloys. *Surface Coatings Technology*, 397.

37 Matykina, E., Arrabal, R., Skeldon, P., Thompson, G. E., Wang, P., & Wood, P. 2010. Plasma electrolytic oxidation of a zirconium alloy under AC conditions. *Surface Coatings Technology*, 204(14), 2142–2151.

38 Zhu, L., Zhang, W., Liu, H., Liu, L., Wang, F., & Qiao, Z. 2022. Single dense layer of PEO coating on aluminum fabricated by 'chain-like' discharges. *Materials*, 15(13).

39 Jangde, A., Kumar, S., & Blawert, C. 2020. Evolution of PEO coatings on AM50 magnesium alloy using phosphate-based electrolyte with and without glycerol and its electrochemical characterization. *Journal of Magnesium and Alloys*, 8(3), 692–715.

40 Clyne, T. W., & Troughton, S. C. 2019. A review of recent work on discharge characteristics during plasma electrolytic oxidation of various metals. *International Materials Reviews*, 64(3), 127–162.

41 Ntomprougkidis, V., Martin, J., Nominé, A., & Henrion, G. 2019. Sequential run of the PEO process with various pulsed bipolar current waveforms. *Surface Coatings Technology*, 374, 713–724.

42 Tsai, D. S., & Chou, C. C. 2018. Review of the soft sparking issues in plasma electrolytic oxidation. *Metals*, 8(2).

43 Rogov, A. B., Yerokhin, A., & Matthews, A. 2017. The role of cathodic current in plasma electrolytic oxidation of aluminum: Phenomenological concepts of the 'soft sparking' mode. *Langmuir*, 33(41), 11059–11069.

44 Cheng, Y., Matykina, E., Arrabal, R., Skeldon, P., & Thompson, G. E. 2012. Plasma electrolytic oxidation and corrosion protection of Zircaloy-4. *Surface Coatings Technology*, 206(14), 3230–3239.

45 Cheng, Y., et al. 2012. Comparison of plasma electrolytic oxidation of zirconium alloy in silicate- and aluminate-based electrolytes and wear properties of the resulting coatings. *Electrochimica Acta*, 85, 25–32.

46 Rogov, A. B., Matthews, A., & Yerokhin, A. 2020. Relaxation kinetics of plasma electrolytic oxidation coated Al electrode: Insight into the role of negative current. *Journal of Physical Chemistry C*, 124(43), 23784–23797.

47 Savushkina, S., Gerasimov, M., Apelfeld, A., & Suminov, I. 2021. Study of coatings formed on zirconium alloy by plasma electrolytic oxidation in electrolyte with submicron yttria powder additives. *Metals*, 11(9).

48 Cheng, Y. L., Xue, Z. G., Wang, Q., Wu, X. Q., Matykina, E., Skeldon, P., & Thompson, G. E. 2013. New findings on properties of plasma electrolytic oxidation coatings from study of an Al–Cu–Li alloy. *Electrochimica Acta, 107*, 358-378.

49 Li, N., Yuan, K., Song, Y., Cao, J., Xu, L., & Xu, J. 2021. Plasma electrolytic oxidation of Zircaloy-2 alloy in potassium hydroxide/sodium silicate electrolytes: The effect of silicate concentration. *Bol. la Soc. Esp. Ceram. y Vidr.*, 60(5), 328–336.

50 Yi, A., Liao, Z., Zhu, W., Zhu, Z., Li, W., Li, K., ... & Huang, S. 2020. Influence of electrolyte temperature on the color values of black plasma electrolytic oxidation coatings on AZ31B Mg alloy.

51 Muhammad, F. H., Saaid, F. I., Razamin, N. A. Y., & Winie, T. 2017. Effect of temperature on conductivity performance of PEO-NaI based polymer electrolytes. *Advanced Materials Research*, 1142(1), 128–133.

52 Luo, S., Wang, Q., Ye, R., & Ramachandran, C. S. 2019. Effects of electrolyte concentration on

the microstructure and properties of plasma electrolytic oxidation coatings on Ti-6Al-4V alloy. *Surface Coatings Technology*, 375, 864–876.

53 Hussein, R. O., Nie, X., & Northwood, D. O. 2019. Effect of current mode on the plasma discharge, microstructure and corrosion resistance of oxide coatings produced on 1100 aluminum alloy by plasma electrolytic oxidation. *WIT Transactions on Engineering Science*, 124, 3–16.

54 Jadhav, P., Bongale, A., & Kumar, S. 2021. The effects of processing parameters on the formation of oxide layers in aluminium alloys using plasma electrolytic oxidation technique. *Journal of Mechanical Behavior of Materials*, 30(1), 118–129.

55 Sikdar, S., Menezes, P. V., Maccione, R., Jacob, T., & Menezes, P. L. 2021. Plasma electrolytic oxidation (PEO) process—processing, properties, and applications. *Nanomaterials*, 11(6), 1–42.

56 Zhang, Y., Chen, Y., Duan, X., & Zhao, Y. 2021. Effect of treatment time on a PEO-coated AZ31 magnesium alloy. *Materials and Corrosion*, 72(12), 1885–1893.

57 Egorkin, V. S., Gnedenkov, S. V., Sinebryukhov, S. L., Vyaliy, I. E., Gnedenkov, A. S., & Chizhikov, R. G. 2018. Increasing thickness and protective properties of PEO-coatings on aluminum alloy. *Surface Coatings Technology*, 334, 29–42.

58 Rakoch, A. G., et al. 2020. Plasma electrolytic oxidation of AZ31 and AZ91 magnesium alloys: Comparison of coatings formation mechanism. *Journal of Magnesium and Alloys*, 8(3), 587–600.

59 Wu, T., et al. 2022. Role of phosphate, silicate and aluminate in the electrolytes on PEO coating formation and properties of coated Ti6Al4V alloy. *Applied Surface Science*, 595, 153523.

60 Casanova, L., Ceriani, F., Pedeferri, M., & Ormellese, M. 2022. Addition of organic acids during PEO of titanium in alkaline solution. *Coatings*, 12(2).

61 Morgenstern, R., Sieber, M., & Lampke, T. 2016. Plasma electrolytic oxidation of AMCs. *IOP Conference Series: Materials Science and Engineering*, 118(1), 012031.

62 Zhuanga, J., Song, R., Xiang, N., Lu, J., & Xiong, Y. 2017. Effects of oxidation time on corrosion resistance of plasma electrolytic oxidation coatings on magnesium alloy. *International Journal of Materials Research*, 108(9), 758–766.

63 Tavares, M. D. M., et al. 2019. Effect of duty cycle and treatment time on electrolytic plasma oxidation of commercially pure Al samples. *Journal of Materials Research and Technology*, 8(2), 2141–2147.

64 Simchen, F., Sieber, M., Kopp, A., & Lampke, T. 2020. Introduction to plasma electrolytic oxidation—an overview of the process and applications. *Coatings*, 10(7).

65 Hussein, R. O. 2010. Study on electrolytic plasma discharging behavior and its influence on the plasma electrolytic oxidation coatings.

66 Brown, S. D., Kuna, K. J., & Van, T. B. 1971. Anodic spark deposition from aqueous solutions of NaAlO2 and Na2SiO3. *Journal of the American Ceramic Society*, 54(8), 384–390.

67 Hussein, R. O., Nie, X., & Northwood, D. O. 2015. Plasma electrolytic oxidation (PEO) coatings on Mg-alloys for improved wear and corrosion resistance. In *Surface Contact Mechanics Including Tribology XII* (1), 163–176.

68 Cui, S., Han, J., Du, Y., & Li, W. 2007. Corrosion resistance and wear resistance of plasma electrolytic oxidation coatings on metal matrix composites. *Surface Coatings Technology*, 201(9-11 SPEC. ISS.), 5306–5309.

69 Mengesha, G. A., Chu, J. P., Lou, B. S., & Lee, J. W. 2020. Corrosion performance of plasma electrolytic oxidation grown oxide coating on pure aluminum: Effect of borax concentration. *Journal of Materials Research and Technology*, 9(4), 8766–8779.

70 Peng, Z., Xu, H., Liu, S., Qi, Y., & Liang, J. 2021. Wear and corrosion resistance of plasma electrolytic oxidation coatings on 6061 Al alloy in electrolytes with aluminate and phosphate. *Materials*, 14(14).

71 Molaei, M., Babaei, K., & Fattah-alhosseini, A. 2021. Improving the wear resistance of plasma electrolytic oxidation (PEO) coatings applied on Mg and its alloys under the addition of nano- and micro-sized additives into the electrolytes: A review. *Journal of Magnesium and Alloys*, 9(4), 1164–1186.

72 Li, J., Bai, X., Zhang, D., & Li, H. 2006. Characterization and structure study of the anodic oxide film on Zircaloy-4 synthesized using NaOH electrolytes at room temperature. *Applied Surface Science*, 252(20), 7436–7441.

73 Pauporté, T., Finne, J., Kahn-Harari, A., & Lincot, D. 2005. Growth by plasma electrolysis of

zirconium oxide films in the micrometer range. *Surface Coatings Technology*, 199(2-3 SPEC. ISS.), 213–219.

74 Chen, Y., Nie, X., & Northwood, D. O. 2010. Plasma electrolytic oxidation (PEO) coatings on a zirconium alloy for improved wear and corrosion resistance. University of Windsor.

75 Hui, Z., Zhengxian, L., & Jihong, D. (2005). Oxide coatings on zirconium alloy deposited by AC microarc oxidation. *Rare Metals Materials and Engineering*, 34(8), 1330.

76 Matykina, E., Arrabal, R., Skeldon, P., Thompson, G. E., Wang, P., & Wood, P. 2010. Plasma electrolytic oxidation of a zirconium alloy under AC conditions. *Surface and Coatings Technology*, 204(14), 2142–2151.

77 Xue, W., Zhu, Q., Jin, Q., & Hua, M. 2010. Characterization of ceramic coatings fabricated on zirconium alloy by plasma electrolytic oxidation in silicate electrolyte. *Materials Chemistry and Physics*, 120(2-3), 656–660.

78 Chen, Y., Nie, X., & Northwood, D. O. 2010. Investigation of plasma electrolytic oxidation (PEO) coatings on a Zr-2.5Nb alloy using high temperature/pressure autoclave and tribological tests. *Surface Coatings Technology*, 205(6), 1774–1782.

79 Matykina, E., Arrabal, R., Skeldon, P., & Thompson, G. E. 2010. Optimisation of the plasma electrolytic oxidation process efficiency on aluminium. *Surface and Interface Analysis*, 42(4), 221–226.

80 Wang, Y. M., Feng, W., Xing, Y. R., Ge, Y. L., Guo, L. X., Ouyang, J. H., ... & Zhou, Y. 2018. Degradation and structure evolution in corrosive LiOH solution of microarc oxidation coated Zircaloy-4 alloy in silicate and phosphate electrolytes. *Applied Surface Science*, *431*, 2-12.

81 Li, N., Yuan, K., Song, Y., Cao, J., Xu, L., & Xu, J. 2020. Plasma electrolytic oxidation of Zircaloy-2 alloy in potassium hydroxide/sodium silicate electrolytes: The effect of silicate concentration. *Bol. la Soc. Esp. Ceram. y Vidr.*

82 Cheng, Y. L., & Wu, F. 2012. Plasma electrolytic oxidation of zircaloy-4 alloy with DC regime and properties of coatings. *Trans. Nonferrous Met. Soc. China (English Ed.)*, *22*(7), 1638–1646.

83 Rokosz, K., et al. 2019. SEM, EDS and XPS studies of AC & DC PEO coatings obtained on titanium substrate. *IOP Conf. Ser. Mater. Sci. Eng.*, *564*(1).

84 Fatkullin, A. R., Parfenov, E. V., Yerokhin, A., Lazarev, D. M., & Matthews, A. 2015. Effect of positive and negative pulse voltages on surface properties and equivalent circuit of the plasma electrolytic oxidation process. *Surf. Coatings Technol.*, *284*, 427–437.

85 Toro, L., Zuleta, A. A., Correa, E., Calderón, D., Galindez, Y., Calderón, J., ... & Valencia-Escobar, A. 2020. New insights on the influence of low frequency pulsed current on the characteristics of PEO coatings formed on AZ31B. *Materials Research Express*, *7*(1), 016539.Gao, Y., Yerokhin, A., & Matthews, A. 2014. Effect of current mode on PEO treatment of magnesium in Ca- and P-containing electrolyte and resulting coatings. *Appl. Surf. Sci.*, *316*, 558–567.

86 Fattah-alhosseini, A., Chaharmahali, R., Keshavarz, M. K., & Babaei, K. 2021. Surface characterization of bioceramic coatings on Zr and its alloys using plasma electrolytic oxidation (PEO): A review. *Surfaces and Interfaces*, *25*.

87 Bahador, R., Hosseinabadi, N., & Yaghtin, A. 2021. Effect of power duty cycle on plasma electrolytic oxidation of A356-Nb2O5 metal matrix composites. *J. Mater. Eng. Perform.*, *30*(4), 2586–2604.

88 Arrabal, R., Mohedano, M., Mingo, B., Matykina, E., Pardo, A., & Merino, M. C. 2015. Characterization and corrosion behaviour of PEO coatings on AM50 magnesium alloy with incorporated particles. In *European Corrosion Congress, EUROCORR 2015* (3), 1924–1933.

89 Tang, Q., & Gong, J. 2013. Effect of porosity on the microhardness testing of brittle ceramics: A case study on the system of NiO-ZrO2. *Ceram. Int.*, *39*(8), 8751–8759.

90 Zhuang, J. J., Song, R. G., Xiang, N., Xiong, Y., & Hu, Q. 2017. Effect of current density on microstructure and properties of PEO ceramic coatings on magnesium alloy. *Surf. Eng.*, *33*(10), 744–752.

91 Dehnavi, V., Luan, B. L., Shoesmith, D. W., Liu, X. Y., & Rohani, S. 2013. Effect of duty cycle and applied current frequency on plasma electrolytic oxidation (PEO) coating growth behavior. *Surf. Coatings Technol.*, *226*, 100–107.

92 Attarzadeh, N., & Ramana, C. V. (2021. Plasma electrolytic oxidation ceramic coatings on

zirconium (Zr) and zirconium alloys: Part I—Growth mechanisms, microstructure, and chemical composition. *Coatings*, *11*(6).

93 Sabouri, M., Mousavi Khoei, S. M., & Neshati, J. 2017. Plasma current analysis using discrete wavelet transform during plasma electrolytic oxidation on aluminum. *J. Electroanal. Chem.*, *792*, 79–87.